Journal of Cancer Research and Clinical Oncology (2022) 148:1073–1085
https://doi.org/10.1007/s00432-021-03899-7

ORIGINAL ARTICLE – CANCER RESEARCH

In vivo and in vitro inhibition of SCLC by combining dual cancer-specific recombinant adenovirus with Etoposide

Tingyu Li[1,2] · Jinbo Fang[1,2] · Jihao Chu[3] · Xing Liu[4] · Yiquan Li[1,2] · Yilong Zhu[1,2] · Shanzhi Li[1,2] · Zhiru Xiu[1] · Yaru Li[1] · Ningyi Jin[1,2,5] · Guangzhe Zhu[1] · Lili Sun[6] · Xiao Li[1,2,5]

Received: 9 September 2021 / Accepted: 21 December 2021 / Published online: 17 January 2022

Abstract

Purpose Oncolytic virotherapy is emerging as an important modality in cancer treatment. In a previous study, we designed and constructed Ad-Apoptin-hTERTp-E1a (Ad-VT), a dual cancer-selective anti-tumor recombinant adenovirus.

Methods To explore the therapeutic effect of recombinant adenovirus Ad-VT together with Etoposide on small cell lung cancer, the ability of Ad-VT alone, Etoposide alone, and a combination of Ad-VT + Etoposide to inhibit proliferation of NCI-H446 and BEAS-2B cells was investigated using the WST-1 method. According to the inhibitory action of different combinations, a combination index (CI) was estimated by CalcuSyn software to select the best combination. The inhibitory effect of Ad-VT combined with Etoposide on NCI-H446 and BEAS-2B cells was detected by crystal violet staining and the CFST method. Hoechst, Annexin V and JC-1 staining were used to explore the inhibitory pathway of Ad-VT combined with Etoposide on NCI-H446 cells. The migratory and invasive abilities of treated NCI-H446 cells were assessed by Transwell and BioCat methods. Tumor volume, body weight and survival rate were measured to analyze the anti-tumor and toxic effects of different treatments in tumor-bearing mice.

Results Ad-VT (20 MOI) combined with Etoposide (400 nM) significantly inhibited NCI-H446 cell proliferation with reduced toxicity of Etoposide to normal cells. Ad-VT induced apoptosis of NCI-H446 cells mainly through the mitochondrial apoptosis pathway, an effect significantly increased by the combined treatment. Ad-VT together with Etoposide significantly inhibited migration and invasion of NCI-H446 cells, inhibited tumor growth in vivo and prolonged the survival of tumor-bearing mice.

Conclusions The above results indicate that when combined with Etoposide, Ad-VT may have an important role in synergistically inhibiting tumors.

Keywords Recombinant adenovirus · Etoposide · Small cell lung cancer · Synergy

Tingyu Li and Jinbo Fang have contributed equally to this work.

✉ Guangzhe Zhu
zhuguangze820@126.com

✉ Lili Sun
linjiaxiaoya@163.com

✉ Xiao Li
lixiao06@mails.jlu.edu.cn

[1] Academician Workstation of Jilin Province, Changchun University of Chinese Medicine, Jingyue Economic and Technological Development Zone, No. 1035, Boshuo Road, Changchun 130117, Jilin, People's Republic of China

[2] Changchun Veterinary Research Institute, Chinese Academy of Agricultural Sciences, Changchun 130122, People's Republic of China

[3] College of Life Sciences, Jilin University, Changchun 130012, People's Republic of China

[4] Department of Thoracic Surgery, The First Hospital of Jilin University, Changchun 130012, People's Republic of China

[5] Jiangsu Co-Innovation Center for Prevention and Control of Important Animal Infectious Diseases and Zoonoses, Yangzhou 225009, People's Republic of China

[6] Department of Head and Neck Surgery, Tumor Hospital of Jilin Province, Changchun 130012, People's Republic of China

Introduction

Cancer is a leading global cause of death in the twenty-first century, and its incidence is rapidly rising. Lung cancer has the highest incidence and mortality rate, accounting for 11.6% and 18.4%, respectively (Sung et al. 2020). From the perspective of pathology, lung cancer can be divided into small cell lung cancer (SCLC) and non-small cell lung cancer (NSCLC). SCLC is a highly malignant tumor, which is sensitive to radiotherapy and chemotherapy, and has a high metastasis rate. Lymph node and blood metastases often occur in the early stage.

At present, the most common treatment for SCLC is surgery combined with radiotherapy and chemotherapy (such as Etoposide, irinotecan, topotecan, gemcitabine, and paclitaxel). However, surgical treatment is limited to early-stage patients and has a poor efficacy. Although SCLC is sensitive to chemotherapy drugs, these have significant side effects, leading to a general decline in the quality of life. Treatment is often discontinued due to inability to tolerate the chemotherapy. With the development of molecular biology, cell biology and virology, gene therapy has become a new method for the treatment of cancer. Oncolytic viruses have notable advantages, having dual functions of viral therapy and gene therapy, and are expected to become an effective method for treating SCLC (Gu et al. 2009).

Oncolytic viruses (OVs) can be used not only as oncolytic agents, but also as effective carriers of anti-cancer genes and are promising anti-tumor agents. On the one hand, OVs can selectively replicate in tumor cells and effectively kill them by introducing anti-cancer genes without damaging normal cells. On the other hand, cancer cells can be killed indirectly through immune-mediated cancer cell clearance pathways or tumor vessel targeting. Some viruses, such as adenovirus, herpes simplex virus, vaccinia virus, respiratory enterovirus and vesicular stomatitis virus etc. have been used as oncolytic agents (Chiocca and Rabkin 2014). Of these, adenoviruses are the most widely studied and it has been confirmed that oncolytic adenoviruses has good anti-tumor effects and safety profiles (Fulci and Chiocca 2003; Chiocca et al. 2004; Kemeny et al. 2006). At present, oncolytic adenoviruses have been developed for the treatment of cancer together with drugs (Sato-Dahlman and Yamamoto 2018).

Apoptin, derived from chicken anemia virus with single negative strand DNA (Sato-Dahlman and Yamamoto 2018; Noteborn et al. 1991; Noteborn and Koch 1995; Phenix et al. 1994), is a VP3 protein that can induce apoptosis. It is 14 kD in size and rich in proline, serine, threonine and basic amino acids. Apoptin has the ability to selectively kill a variety of human tumor or abnormal transformed cells, but is not cytotoxic to normal cells (Noteborn et al. 1994). Apoptin contains two nuclear localization sequences (NLS) across the C-terminal of amino acids 82–88 (NLS1) and 111–121 (NLS2), which help proteins shuttle between the nucleus and cytoplasm. It also contains several potential threonine and serine phosphorylation sites, such as Thr-108 at the C-terminal. Thr-108 is phosphorylated in cancer cells, but not in normal cells (Heilman et al. 2006; Danen-Van Oorschot et al. 2003; Rohn et al. 2002).

Telomerase is a ribonuclease with reverse transcriptase activity. As the rate-limiting component of telomerase, human telomerase reverse transcriptase (hTERT) plays a decisive role in the activity of telomerase (Zhang et al. 2015). Most normal human cells lack telomerase activity, but high hTERT expression and telomerase activation can be observed in most human malignant tumors, imbuing cancer cells with acquired unlimited proliferation ability (Qian et al. 2014). Studies have shown that many targeted anticancer genes rely on hTERT promoter blockade with high efficiency and specificity, which offers a new method for cancer treatment. In earlier work, we constructed a recombinant adenovirus (Ad-Apoptin-hTERTp-E1a, Ad-VT) which can specifically kill tumor cells using the characteristics of Apoptin and hTERT (Xiao et al. 2010). Ad-VT selectively recognizes and infects cancer cells, and replicates in large numbers therein. At the same time, it expresses Apoptin, which eventually leads to cancer cell death. Another study has shown that the recombinant adenovirus has significant cytotoxicity for several other tumor cells (Liu et al. 2012; Qi et al. 2014; Yang et al. 2015; Zhang et al. 2013).

In the present study, Ad-VT was combined with Etoposide to determine the optimal combination concentration in in vivo and in vitro experiments, to reduce the toxicity of Etoposide and improve the therapeutic effect on SCLC.

Materials and methods

Cells and viruses

The SCLC cell line (NCI-H446) and the human lung normal bronchial epithelial cell line (BEAS-2B) were purchased

Fig. 1 Schematic diagram and synergistic analysis of Ad-VT combined with Etoposide. **A** Schematic diagram of two recombinant adenovirus vectors. (a) Ad-Apoptin-hTERTp-E1a (Ad-VT). Ad-VT contains the hTERT promoter, E1a gene and Apoptin gene. (b) Ad-Mock. Ad-Mock does not contain other foreign genes. **B** WST-1 assay measuring the inhibition of Ad-VT, Etoposide and a combination of the two on NCI-H446 cells at 24, 48, and 72 h. **C** WST-1 assay measuring the inhibition of Ad-VT, Etoposide and the combination on BEAS-2B cells at 24, 48, and 72 h. **D** The combination index of Ad-VT and Etoposide on NCI-H4466 cells was calculated by CalcuSyn software. Data are representative of three independent experiments. Unpaired Student's *t* test: $*P<0.05$, $**P<0.01$, $***P<0.001$ ▶

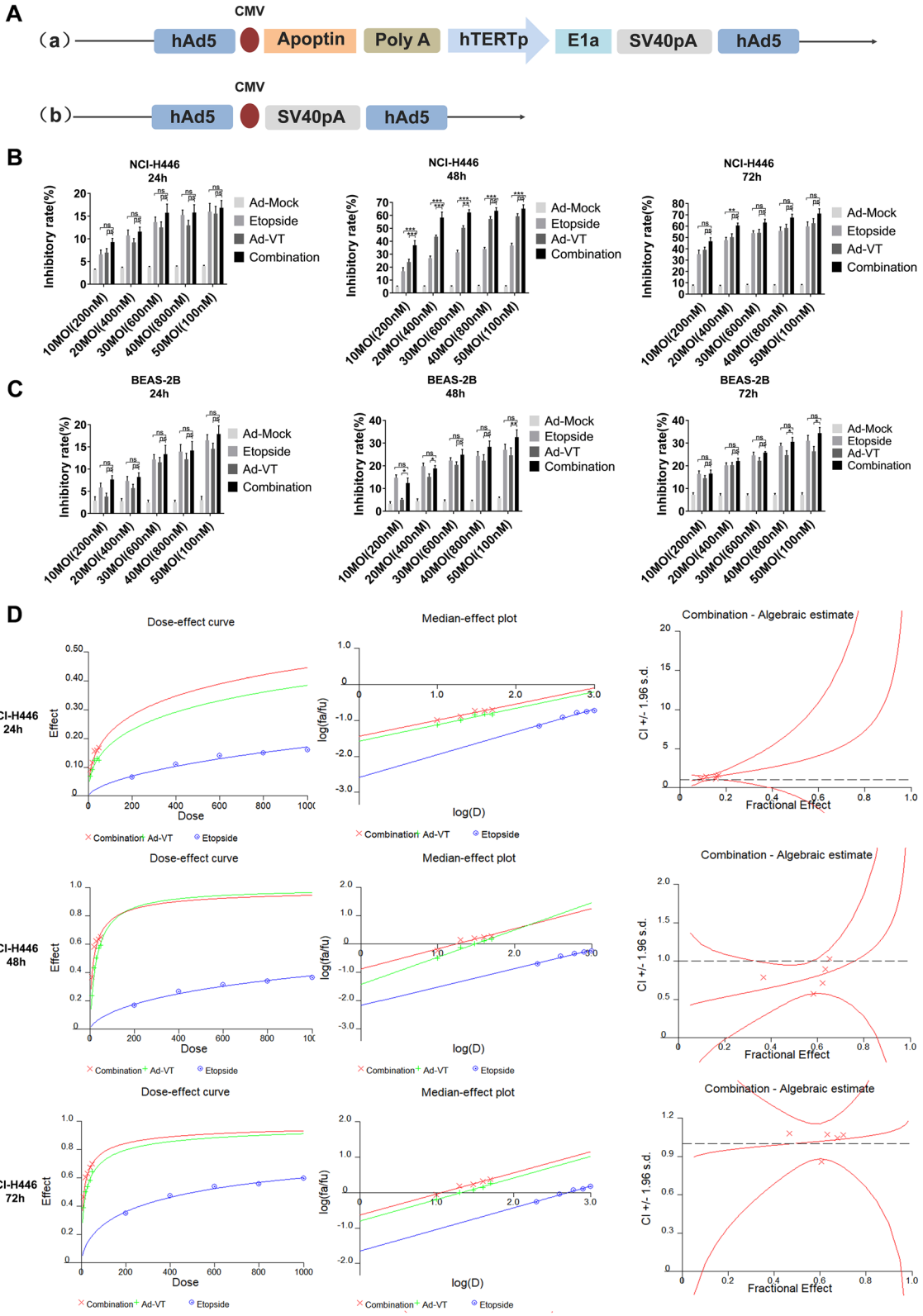

from the Chinese Academy of Sciences (Shanghai cell bank). The NCI-H446 cells were cultured in RPMI 1640 medium, The BEAS-2B cells were cultured in DMEM medium. 10% fetal bovine serum (FBS), 50 U/mL penicillin and 50 U/mL streptomycin were added and cells were cultured in a 37 °C incubator containing 5% carbon dioxide. All cell culture

reagents were purchased from HyClone, GE Healthcare, and Life Sciences. The recombinant adenoviruses Ad-Apoptin-hTRETp-E1a (Ad-VT) and Ad-Mock were constructed and maintained in our laboratory (Fig. 1A) (Xiao et al. 2010). We used the ViraTrap™ Adenovirus Purification Maxiprep kit (BIOMIGA) to purify the recombinant adenovirus Ad-VT and Ad-Mock. Subsequently, HEK-293 cells were used to determine the virus titer. The HEK-293 cells were cultured in 96-well plates at a density of 5×10^3 cells/well. The purified recombinant adenovirus was diluted 10^{-1}–10^{-12} and added to the 96-well plate with eight replicate wells for each gradient. Continue to incubate for 5 days. After 5 days, observe the number of cytopathic wells and use Reed and Muench's method to calculate (Reed and Muench 1938).

Experimental animals

Female BALB/c nude mice (4–5 weeks old) were purchased from Beijing vital River Laboratory Animal Technology Co., Ltd., and the experimental protocols were approved by the Institutional Animal Care and Use Committee (IACUC) of Changchun University of Chinese Medicine. All surgeries were performed under anesthesia with sodium pentobarbital, and all efforts were made to minimize suffering. After the experiment, the remaining mice were euthanized by intraperitoneal injection of three times the anesthetic dose of sodium pentobarbital (150 mg/kg) for 2–3 min. The euthanasia method followed the AVMA Guidelines for the Euthanasia of Animals.

Determination of cytotoxic synergy

The NCI-H446 and BEAS-2B cells were cultured in 96-well plates at a density of 5×10^3 cells/well. After 24 h, Ad-VT and Etoposide (alone or in combination) were added at 24, 48, and 72 h, after which 10 µL WST-1 solution was mixed with 90 µL serum-free medium and added to each well for 90 min at 37 °C. Subsequently, absorbance was measured by Microplate Reader. The cell proliferation inhibition rate was calculated as follows:

$$\text{Cell inhibition rate} = 100\% \times \left[1 - \text{OD (absorbance of treated wells)}/\text{OD(absorbance of control wells)}\right].$$

The combination index (CI) values were calculated from the CI equation algorithms using CalcuSyn software analyses (Biosoft v2.0). CI = 1, < 1 and > 1 indicate additive, synergistic and antagonistic effects, respectively. The optimal combination of dose and time were screened by CI index and inhibition rate of each combination.

Cell inhibition assays

Inhibition of proliferation of NCI-H446 and BEAS-2B cells was detected by crystal violet staining and the CFST method. The NCI-H446 and BEAS-2B cells were cultured in 12-well plates at a density of 2×10^5 cells/well at 37 °C and 5% CO_2 for 24 h. Blank control, Ad-Mock (20 MOI), Etoposide (400 nM), Ad-VT (20 MOI) and Ad-VT (20 MOI) + Etoposide (400 nM) groups were cultured for 48 h after which 0.4% crystal violet solution was added to each well for 5 min. The dye solution was then washed away three times with PBS and images captured.

After staining with CFST, NCI-H446 cells and BEAS-2B cells were placed in a 6-well plate at a density of 2.5×10^5 cells/well. After 24 h culture, blank control, Ad-Mock (20 MOI), Etoposide (400 nM), Ad-VT (20 MOI) and Ad-VT (20 MOI) + Etoposide (400 nM) groups were cultured for 48 h, after which the inhibition in each treatment group was assessed by flow cytometry.

Measurement of apoptosis in SCLC

Hoechst and Annexin V staining methods were used to determine the effects of Ad-VT or Etoposide alone or in combination on apoptosis of SCLC, and Western blotting was used for verification.

NCI-H446 cells were cultured at 2.5×10^5 cells/well in 6-well cell culture plates, which were pre-inserted with cover slips, for 24 h. Blank controls, Ad-Mock, Etoposide, Ad-VT and Ad-VT + Etoposide groups were cultured at the same concentrations as above for 48 h, after which they were washed × 3 times with PBS. 1 mL of Hoechst dye (1:1000) was added to each well and the plates were incubated at 37 °C for 8 min. Thereafter, the cover slips were washed twice with PBS and then examined and photographed under a fluorescence microscope.

NCI-H446 cells were cultured in a 6-well plate at a density of 2.5×10^5 cells/well for 24 h. The above five experimental groups were treated for 48 h, followed by harvesting the cells and washing × 3 with PBS. Next, 500 µL of 1 × Annexin V binding buffer was added to each well, followed by 5 µL of FITC solution and 5 µL of PI solution. The cells were incubated at room temperature in the dark for 20 min. Apoptosis was then assessed by flow cytometry. Western blotting was used to verify apoptosis of NCI-H446 cells in each experimental group.

Delineation of apoptosis pathways in SCLC

NCI-H446 cells were cultured for 24 h at 2.5×10^5 cells/well in 6-well cell culture plates, which were pre-inserted with cover slips. The above five experimental groups were cultured for 48 h, after which 1 mL JC-1 staining solution was added to each well for 20 min in the dark. After treatment, the cover slips were washed × 3 with PBS and then observed and photographed under a fluorescence microscope.

NCI-H446 cells were cultured for 24 h in 96-well plates at a density of 5×10^3 cells/well. The above five experimental groups were then treated for 48 h, followed by the addition of 0.1 mL JC-1 staining solution to each well for 20 min in the dark. Finally, absorbance at 435 and 585 nm was determined.

NCI-H446 cells were cultured at 2×10^5 cells/well in 6-well cell culture plates. The above five experimental groups were then treated for 48 h, the cells were harvested and washed × 3 with PBS and then 500 µL of DHR solution was added. Following incubation at room temperature in the dark for 15 min, ROS levels were then determined by flow cytometry. Western blotting was used to verify the apoptosis pathway of NCI-H446 cells in each experimental group.

Cell migration and invasion assay

Transwell method

NCI-H446 cells were prepared as cell suspensions and added to a 12-well plate at a concentration of 1×10^5 cells/mL and cultured for 24 h. The above five experimental groups were analyzed after 48 h of treatment, when the cells were resuspended in 200 µL of serum-free medium and added to the upper chamber. In the lower chamber, 500 µL of culture medium containing 10% serum was added. The cells in the upper layer of the membrane were removed after 24 h. After methanol fixation and crystal violet staining, samples were observed under the microscope and imaged captured. Five fields of view were selected to count cells, repeated three times.

BioCat method

The BioCoat invasion chamber was removed from −20 °C storage and warmed to room temperature. RPMI 1640 serum-free medium was warmed to room temperature. Other methods were as for the Transwell method described above.

Scratch test

NCI-H446 cells were added to a 6-well plate at 1×10^6 cells/well. After 24 h culture, a scratch was made in the cell layer with a sterile microtube and photographed (0 h). The above five experimental groups were cultured for 48 h, after which the width of the scratch was measured and the cell migration rate was calculated. Cell mobility was calculated as follows:

$$\text{Cell mobility} = (\text{0 h scratch width} - \text{48 h scratch width})/\text{0 h scratch width} \times 100\%$$

The migration and invasion of NCI-H446 cells were evaluated by Western blotting.

Tumor inhibition assay in tumor-bearing mice

NCI-H446 cell suspensions (1×10^7 cells/mL) were injected subcutaneously into the right legs of nude mice. After the establishment of the tumor, the mice were randomly divided into six groups, ten mice per group, namely a 1×10^9 PFU/100 µL Ad-VT treatment group, a 5 mg/kg Etoposide treatment group, a 10 mg/kg Etoposide treatment group, a 1×10^9 PFU/100 µL Ad-VT + 5 mg/kg Etoposide treatment group, a 1×10^9 PFU/100 µL Ad-VT + 10 mg/kg Etoposide treatment group and a control group. After successful establishment of this subcutaneous transplantation tumor model in nude mice, treatment with Ad-VT and Etoposide was administered by intra-tumoral and intraperitoneal injection, respectively, every 4 weeks, i.e., Ad-VT was injected into the tumor every 3 days and Etoposide was injected intraperitoneally once a week. The long and short diameters of the xenografted tumors were measured weekly with vernier calipers for 7 weeks. Growth curves were plotted and tumor volume calculated as follows:

$$\text{Tumor volume } (\text{mm}^3) = \left(\text{long diameter of tumor} \times \text{short diameter of tumor}^2\right)/2.$$

Tumor inhibition rate, body weight and survival rate of mice were calculated 4 weeks after drug withdrawal.

Inhibition rate was calculated using the following formula:

$$\text{Tumor inhibition rate} = (1 - \text{treatment group tumor volume}/\text{control tumor volume}) \times 100\%$$

Statistical analysis

Data are presented as mean ± standard error of the mean (SEM). GraphPad Prism 5.0 software was used to perform statistical analyses by unpaired two-tailed Student's *t* tests or analysis of variance (ANOVA). $P < 0.05$ was considered to be statistically significant. $*P < 0.05$, $**P < 0.01$, $***P < 0.001$, $****P < 0.0001$.

Results

WST-1 analysis

NCI-H446 cells were treated with different concentrations of Ad-VT and Etoposide. Ad-VT was used at MOI of 10, 20, 30, 40 and 50 and Etoposide at 200, 400, 600, 800, and 1000 nM. In the combined treatment group, Ad-VT: Etoposide at a ratio of 1:20 was administered. The results of WST-1 showed no significant differences between Ad-VT, Etoposide and combination groups after 24 h of treatment. However, at 48 h, proliferation of NCI-H446 cells in the three groups was inhibited in a dose-dependent manner. Inhibition by a combination of Ad-VT and Etoposide was significantly greater than that of Etoposide alone ($P < 0.001$). Inhibition by 200 nM + 10 MOI, 400 nM + 20 MOI and 600 nM + 30 MOI combinations was significantly greater than that caused by 10 MOI, 20 MOI and 30 MOI Ad-VT ($P < 0.001$). At 72 h, only inhibition by a combination of 400 nM + 20 MOI was significantly different from that of Etoposide (400 nM) or Ad-VT (20 MOI) alone ($P < 0.05$) (Fig. 1B).

The WST-1 method was also used to detect the inhibitory effect of Etoposide, Ad-VT and their combination on BEAS-2B cells. The results showed that there was no significant difference between the effects of single-agent Etoposide and the combination. At 48 h, inhibition in the 400 nM + 20 MOI combination group was significantly less than in the Etoposide 400 nM alone group ($P < 0.05$), indicating that Ad-VT can reduce the cytotoxicity of Etoposide to normal cells. The above results showed that Ad-VT had a strong inhibitory effect on tumor cells. Adding Ad-VT did not increase the inhibitory effects of Etoposide on normal cells, but the combination of Ad-VT and Etoposide had a stronger inhibitory effect on tumor cells (Fig. 1C).

CalcuSyn software analysis

The degree of inhibition of NCI-H446 cells in each treatment group was analyzed by CalcuSyn software (Fig. 1D). This showed that at 48 h, CI < 1 (including 100 nm + 10 MOI, 400 nM + 20 MOI, 600 nM + 30 MOI and 800 nM + 40 MOI groups) indicated synergistic effects, while other treatment groups showed antagonistic effects (CI > 1). After 72 h of treatment, only the 400 nM + 20 MOI group (CI < 1) showed synergistic inhibition.

The same analysis of BEAS-2B cells showed that at 48 h, CI < 1 included 100 nM + 10 MOI, 400 nM + 20 MOI, 600 nM + 30 MOI and 800 nM + 40 MOI groups. Inhibition by the combination of 400 nM + 20 MOI was significantly less than that of Etoposide 400 nm alone ($P < 0.05$).

According to the above results, 400 nM + 20 MOI can reduce toxicity and improve efficiency. Hence, in the following experiments, we used the combination of 400 nM + 20 MOI, with effects assessed at 48 h.

The combination of Ad-VT and etoposide enhances inhibition of SCLC cell proliferation

NCI-H446 and BEAS-2B cells were treated with Ad-Mock, Ad-VT, Etoposide or Ad-VT combined with Etoposide. After 48 h, they were stained with 0.4% crystal violet. From Fig. 2A, we can find that etoposide has a killing effect on both cells, while Ad-VT only has a significant killing effect on NCI-H446 cells, but has no obvious cytotoxic effect on BEAS-2B cells. We also found that the combined use of Ad-VT and etoposide in NCI-H446 cells will significantly increase the killing effect on cells, while the combined use of Ad-VT and etoposide in BEAS-2B cells can reduce the drug Cytotoxic effect on cells.

First, NCI-H446 and BEAS-2B cells were labeled with CFDA-SE dye, and then divided into the four groups Ad-MOCK, Ad-VT, Etoposide, and Ad-VT and Etoposide combined. After 48 h, they were analyzed by flow cytometry. This indicated that proliferation of NCI-H446 cells in the Etoposide, Ad-VT, Ad-VT and Etoposide combination groups was 73.93%, 61.74% and 36.01%, respectively. Thus, proliferation of cells treated with the combination was significantly lower than that of the single-drug group ($P < 0.05$). For BEAS-2B cells, there was no significant difference between combination and the single-drug treatment (Fig. 2B–D). The above results indicate that the combination of Ad-VT and etoposide significantly enhances the inhibitory effect on breast cancer cells over either agent alone, and also reduce the killing of normal cells.

The combination of Ad-VT and etoposide increases apoptosis of NCI-H446 cells

To determine whether Ad-VT and Etoposide promote the apoptosis of NCI-H446 cells, Hoechst staining was used. This showed that the nuclei of NCI-H446 cells treated with Ad-VT 20 MOI, Etoposide 400 nM and a combination of the two (Ad-VT 20 MOI + Etoposide 400 nM) revealed different degrees of bright blue hyperchromatism and fragmentation,

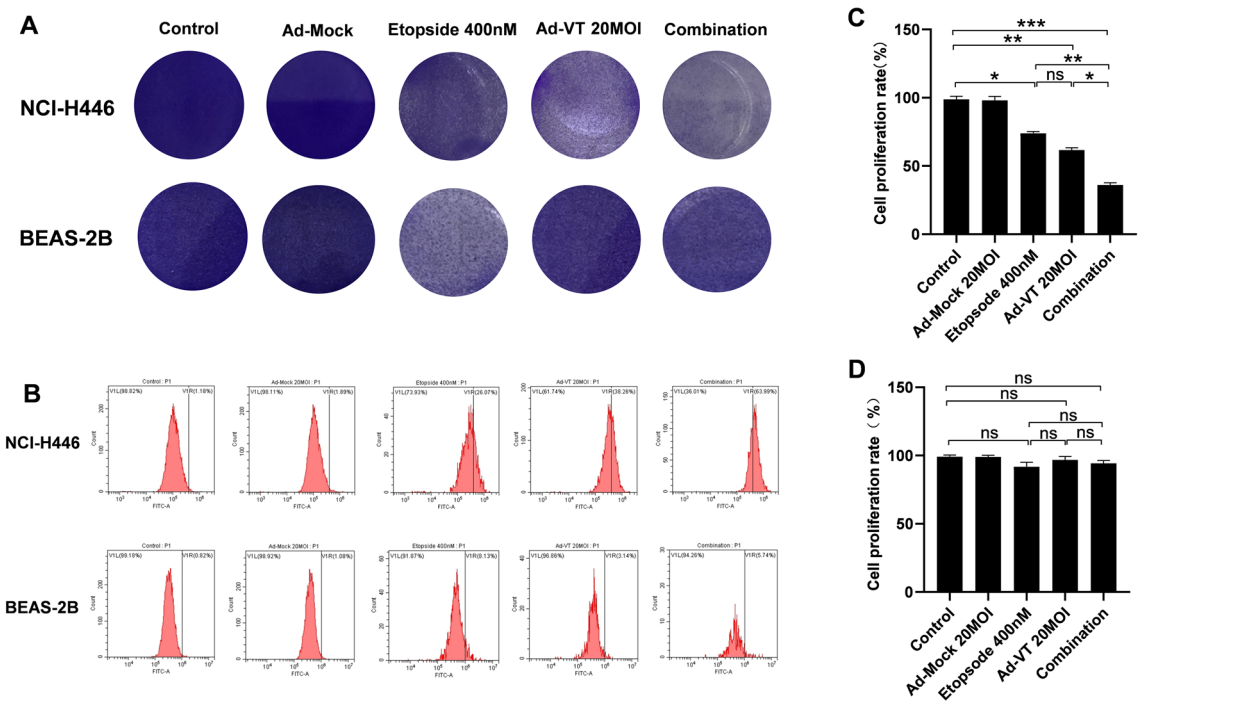

Fig. 2 Inhibitory effect of Ad-VT combined with Etoposide on NCI-H446 and BEAS-2B cells. **A** The inhibitory effects of Ad-VT, Etoposide and their combination on NCI-H446 and BEAS-2B cells were determined by crystal violet staining. **B** Flow cytometry to detect the proliferation of NCI-H446 and BEAS-2B cells after CFSE staining. **C** Proliferation of NCI-H446 cells. **D** Proliferation rate BEAS-2B cells. Data are representative of three independent experiments. Unpaired Student's *t* test: $^{*}P<0.05$, $^{**}P<0.01$, $^{***}P<0.001$

and at the same time, the number of cells showed a downward trend. The effect of the combined treatment was the most notable, while the nuclei of Ad-Mock group showed uniform blue fluorescence (Fig. 3A).

The results of Annexin V-FITC/PI staining showed that Etoposide 400 nM, Ad-VT 20 MOI and the combination (Etoposide 400 nM + Ad-VT 20 MOI) induced apoptosis, but the degree of apoptosis differed between groups. Apoptosis caused by Etoposide 400 nM, Ad-VT 20 MOI and Etoposide 400 nM + Ad-VT 20 MOI was 9.95%, 31.58% and 42.18%, respectively. Thus, inhibition by Ad-VT and the combination treatment NCI-H446 cells was significantly higher than the control group ($P<0.001$), but there was no significant difference between Etoposide and the controls ($P>0.05$) (Fig. 3B, C).

Western blotting results showed that in the Control, Ad-Mock, Etoposide, Ad-VT, and Etoposide + Ad-VT groups, the presence of cleaved PARP and cleaved Caspase-3 proteins gradually increased. These results are consistent with the results of Annexin V-FITC/PI flow cytometry and Hoechst staining, which further confirmed that Etoposide, Ad-VT and the Etoposide + Ad-VT combination inhibited NCI-H446 cell proliferation by inducing apoptosis (Fig. 3D).

Apoptosis pathway of NCI-H446 cells induced by the combination of Ad-VT and etoposide

JC-1 results showed that compared with controls and Ad-Mock treatment, apoptotic cells in the Ad-VT, Etoposide and combination groups increased gradually and along with MMP depolarization, JC-1 gradually changed from red aggregate to green monomer, and the red/green fluorescence ratio decreased gradually. The red/green ratio of the Etoposide group, Ad-VT group and combination group was 0.65, 0.53 and 0.32, respectively, which was significantly lower than that of control group and Ad-Mock group ($P<0.001$). The red/green ratio of the combined group was significantly lower than that of the single-drug group ($P<0.01$) (Fig. 4A, D).

DHR staining was used to detect ROS levels. Compared with the control group and the Ad-Mock group, the levels of ROS in Ad-VT, Etoposide and combination groups were significantly increased ($P<0.001$). The level of ROS in the Ad-VT group was significantly higher than that in Etoposide group ($P<0.001$). The level of ROS in cells treated with the combination was significantly higher than in the Ad-VT group and Etoposide group ($P<0.01$) (Fig. 4B, C).

Western blotting showed that in Control, Ad-Mock, Etoposide, Ad-VT and Etoposide + Ad-VT groups, the

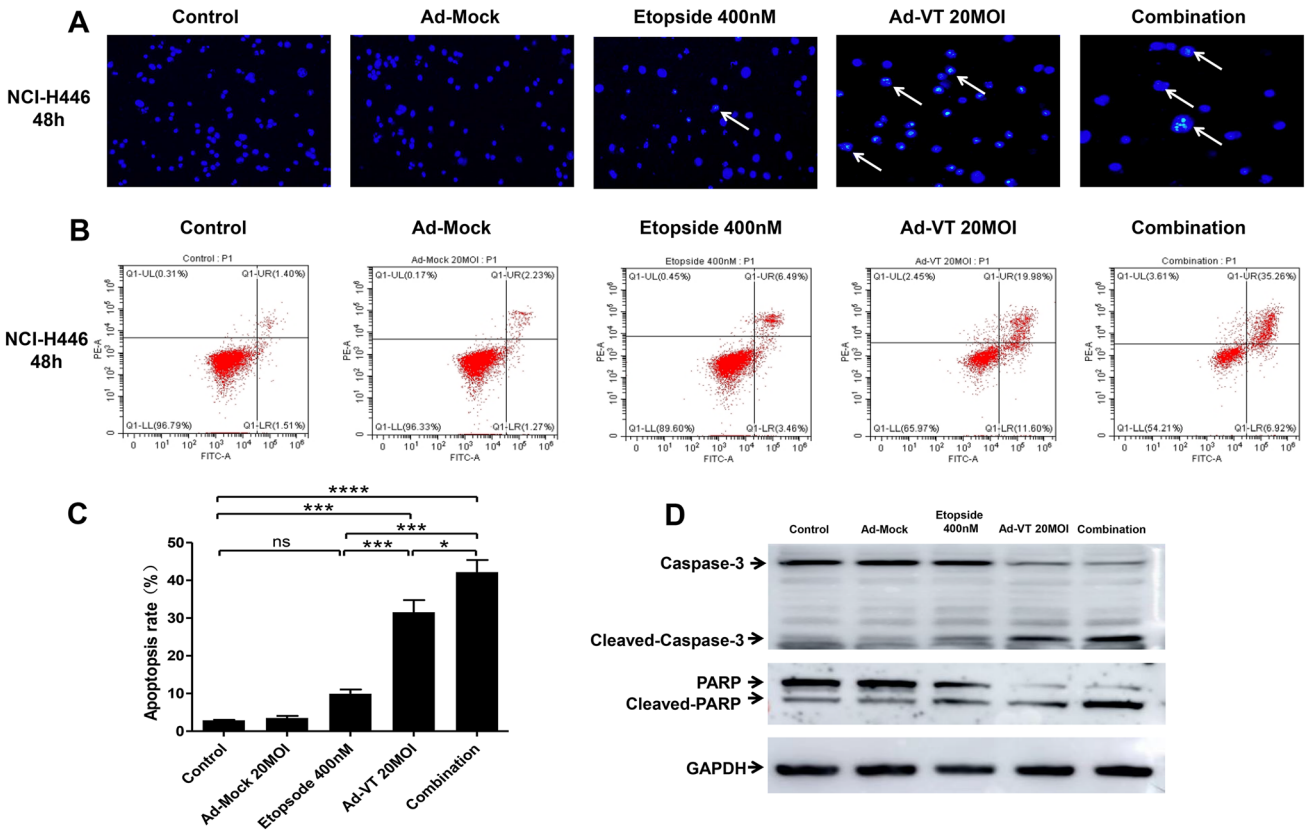

Fig. 3 Apoptosis of NCI-H446 cells induced by Ad-VT combined with Etoposide. **A** Hoechst staining showing nuclei of NCI-H446 cells treated with Ad-VT 20 MOI, Etoposide 400 nM and a combination thereof. **B**, **C** Apoptosis of NCI-H446 cells detected by flow cytometry after Annexin V-FITC/PI staining. Apoptosis was assessed after Ad-VT 20 MOI, Etoposide 400 nM and the combination at 48 h. **D** Western blotting of PARP and Caspase-3 proteins in NCI-H446 cells. Data are representative of three independent experiments. Unpaired Student's *t* test: $^{*}P<0.05$, $^{**}P<0.01$, $^{***}P<0.001$, $^{****}P<0.0001$

presence of cytochrome-c and cleaved-caspase-9 proteins increased gradually. These results suggest that Ad-VT combined with Etoposide induces apoptosis of NCI-H446 cells through mitochondrial membrane potential depolarization (Fig. 4E).

The combination of Ad-VT and etoposide increases the inhibition of NCI-H446 cells migration and invasion

Transwell results showed that the number of migrating cells in the Ad-VT 20 MOI, Etoposide 400 nM and the combination 20 MOI + 400 nM groups was significantly lower than that of the control group ($P<0.001$), indicating that all treatments significantly inhibited the migration of NCI-H446 cells. The number of migrating cells in the combination group was significantly lower than in the single-drug group ($P<0.05$). These results show that the inhibition of migration of NCI-H446 cells by the combination was significantly greater than by a single drug (Fig. 5A, D).

BioCat results showed that the number of invasive cells passing through the basement membrane in Ad-VT 20 MOI, Etoposide 400 nM and 20 MOI + 400 nM combination groups was significantly lower than in the control group ($P<0.001$), indicating that all treatments decreased invasive activity of NCI-H446 cells. The number of invasive cells in the combination group was significantly lower than in the single-drug group ($P<0.05$). These results show that inhibition of invasion of NCI-H446 cells by the combination treatment was significantly greater than by a single drug (Fig. 5B, E). The scratch test showed that the migratory ability of NCI-H446 cells in each treatment group was significantly lower than in the controls ($P<0.01$). Moreover, the migratory ability of cells treated with the combination was significantly lower than with Etoposide or Ad-VT alone ($P<0.01$). The inhibitory effect of Ad-VT on the migration of NCI-H446 cells was significantly higher than with Etoposide alone ($P<0.01$) (Fig. 5C, F).

Western blotting showed that the presence of Vimentin, MMP-2, and MMP-9 proteins decreased gradually, whereas E-cadherin increased gradually in Control, Ad-Mock,

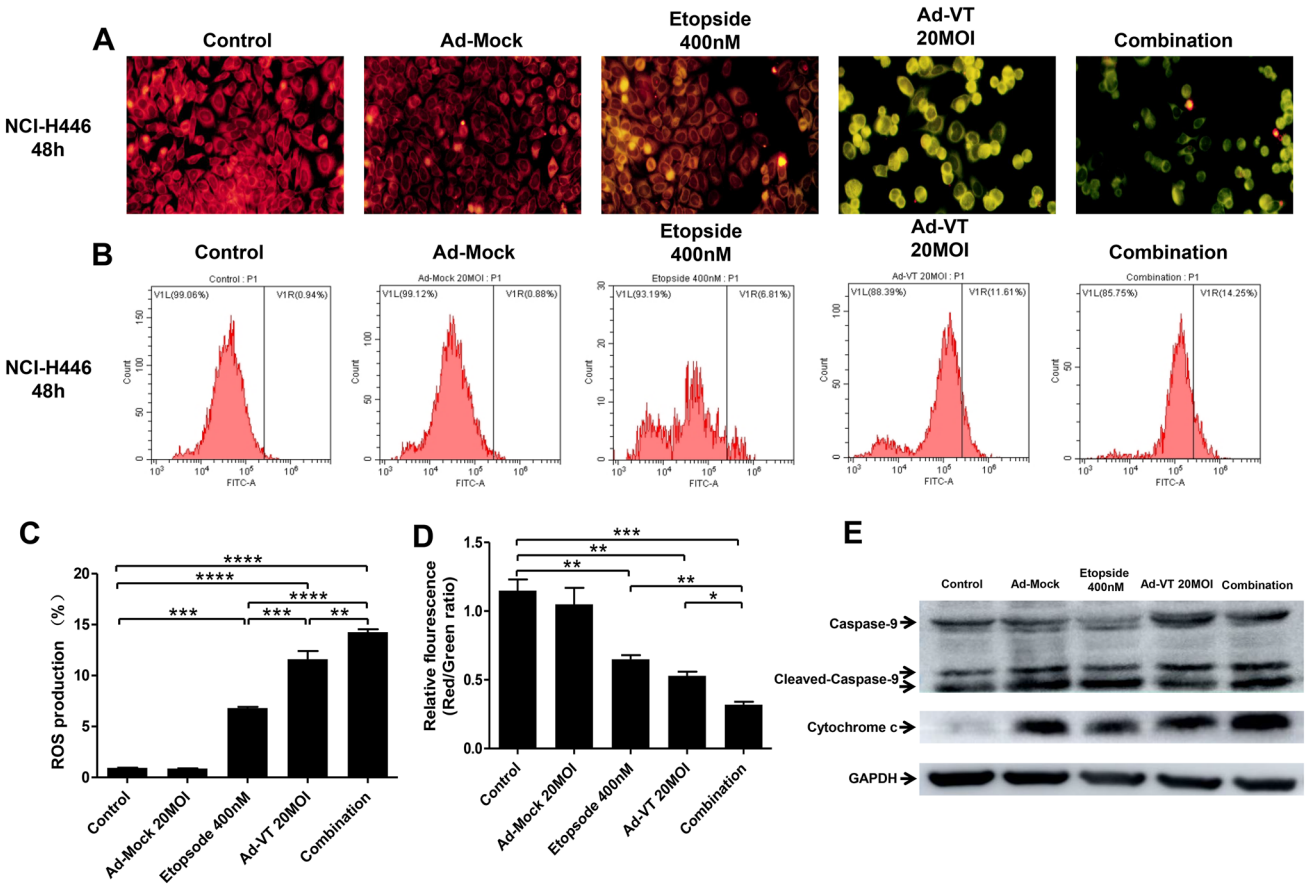

Fig. 4 Apoptosis pathways in NCI-H446 cells induced by Ad-VT combined with Etoposide. **A** Changes of red and green fluorescence of NCI-H446 cells after JC-1 staining observed by fluorescence microscopy. **B**, **C** ROS levels of NCI-H446 cells were detected by flow cytometry after Ad-VT 20 MOI, Etoposide 400 nM and combination treatments at 48 h. **D** Quantitative measurement of changes in the ratio of red to green fluorescence after JC-1 staining. **E** Western blotting of caspase-9 and cytochrome C in NCI-H446 cells. Data are representative of three independent experiments. Unpaired Student's *t* test: $*P<0.05$, $**P<0.01$, $***P<0.001$, $****P<0.0001$

Etoposide, Ad-VT, and combination Etoposide + Ad-VT groups. There was no significant difference between the Ad-Mock and control groups. These results indicate that Ad-VT, Etoposide and the combination inhibited the migration and invasion of NCI-H446 cells and that the inhibitory effect of the combination was stronger than that of a single drug (Fig. 5G).

Anti-tumor effects in vivo

To determine the inhibitory effect of Ad-VT combined with Etoposide on transplanted tumors in mice, tumor size was measured continuously for 7 weeks after establishment of subcutaneous tumor. Animals were treated with Etoposide 5 mg/kg, 10 mg/kg, Ad-VT (1×10^9 PFU), Etoposide 5 mg/kg + Ad-VT (1×10^9 PFU), or the combination Etoposide 10 mg/kg + Ad-VT (1×10^9 PFU). Differences in tumor volumes between treatment and control groups was statistically significant ($P<0.001$). The degree of inhibition in each treatment group was 23.6%, 40.2%, 54.8%, 70%, and 77.5%, respectively (Fig. 6A–C).

Regarding body weights, with time the weight of mice in the control group and Ad-Mock group decreased significantly, while the weight of mice in the Ad-VT, Etoposide and combination groups showed almost no change (Fig. 6D).

A survival analysis of these tumor-bearing mice revealed that the survival rate of mice in the Etoposide 5 mg/kg group and 10 mg/kg group was significantly better than the controls ($P<0.05$). The survival rates of Etoposide 5 mg/kg + Ad-VT (1×10^9 PFU) and Etoposide 10 mg/kg + Ad-VT (1×10^9 PFU) groups were 80% and 100%, respectively, significantly greater than the controls ($P<0.001$) (Fig. 6E).

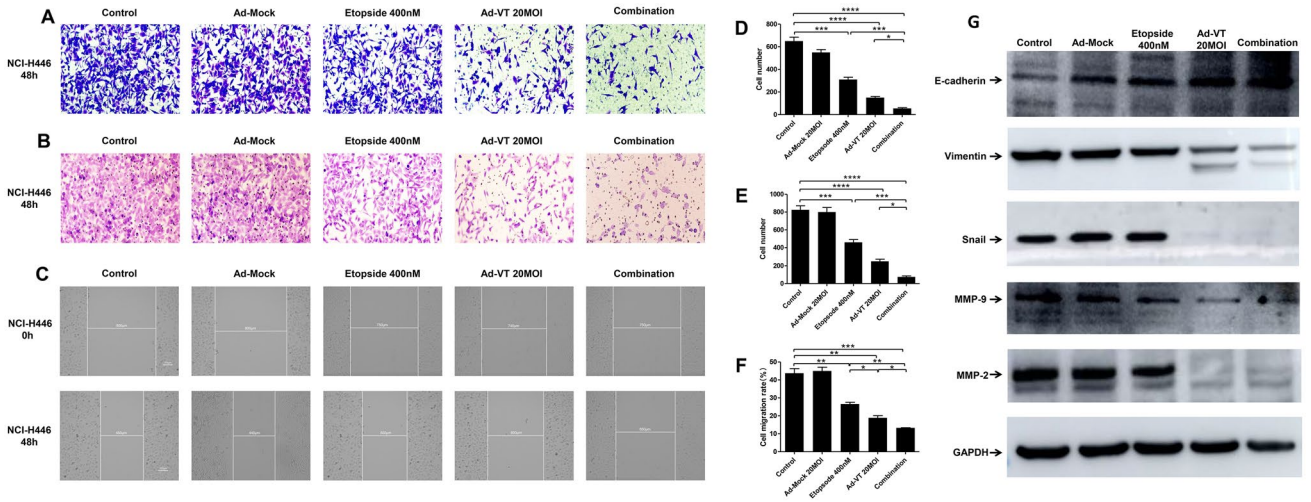

Fig. 5 Effect of Ad-VT combined with Etoposide on migration and invasion of NCI-H446 cells. **A**, **D** Transwell assays detecting the migratory ability of NCI-H446 cells after treatment with Etoposide, Ad-VT, or Etoposide combined with Ad-VT at 48 h. **B**, **E** BioCoat method to test the invasive ability of NCI-H446 cells after Etoposide, Ad-VT, and Ad-VT combined with Etoposide at 48 h. **C**, **F** Scratch test for the migratory ability of NCI-H446 cells after Etoposide, Ad-VT, and Ad-VT combined with Etoposide treatment at 48 h. **G** Western blotting of E-cadherin, Vimentin, Snail, MMP-9 and MMP-2 proteins in NCI-H446 cells. The scale bar equals 100 μm. Cell migration rate = 100% × (scratch width at 0 h − scratch width at 72 h)/scratch width at 0 h. Data are representative of three independent experiments. Unpaired Student's *t* test: $^{*}P<0.05$, $^{**}P<0.01$, $^{***}P<0.001$, $^{****}P<0.0001$

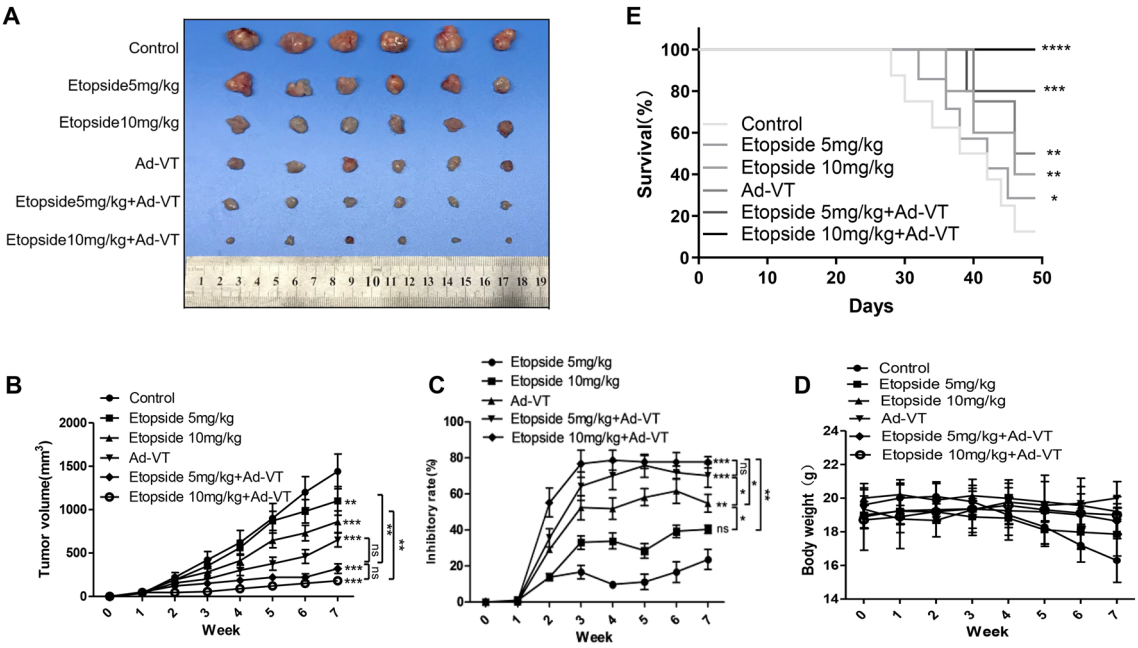

Fig. 6 Effect of Etoposide combined with Ad-VT on SCLC in a BALB/c nude mouse mode. **A–C** Length and width of xenografted tumors measured weekly for 7 weeks using Vernier calipers. The average tumor inhibition was calculated using the formula: (1 − treatment group tumor volume/control tumor volume) × 100%. **D** The weight of tumor-bearing mice was recorded weekly for 7 weeks. **E** The survival rate of tumor-bearing mice was recorded every day for 7 weeks

Discussion

As the second leading global cause of death, cancer incidence rates and mortality are increasing rapidly worldwide, and seriously threatening human health. Among all cancers, the incidence and mortality of lung cancer ranks first (Sung et al. 2020; Bray et al. 2018; Umar et al. 2012; Bade et al. 2020). SCLC is the most malignant lung cancer with occult high invasiveness and rapid progression. Clinical data show that the survival time of patients with SCLC is < 1 year, and the 5-year survival rate is < 7% (Fruh et al. 2013). Currently, treatment of SCLC is still based on chemotherapy. Although this can improve the condition of patients with SCLC, most will relapse due to chemotherapy resistance in a short time (Antonia et al. 2016). Currently, the mechanism of chemotherapy resistance is not clear, and patients will also have serious toxic reactions during chemotherapy. Although some achievements have been made in SCLC molecular targeted therapy, immunotherapy and other precision medicine approaches (Byers and Rudin 2015), most of these studies are still in the stage of clinical second-line or later treatments, and not only are trial sample sizes small, but also the results are inconsistent (Ng et al. 2005).

Recently, with the progress of biomedical and genetic engineering technology, new therapeutic methods have been developed, including oncolytic virotherapy. Oncolytic viruses can specifically infect and replicate in tumor cells and then kill them. Many oncolytic viruses have been tested as oncolytic agents, such as adenoviruses, herpes simplex viruses, vaccinia viruses, respiratory enteroviruses and vesicular stomatitis viruses (Chiocca and Rabkin 2014). Of these, adenoviruses are the most widely studied. A large number of studies have shown that they may offer a very effective strategy to control the specific expression of oncolytic adenovirus genes in tumor cells by inserting tumor-specific promoters. In previous work, our lab constructed a dual specific-cancer recombinant adenovirus (Ad-Apoptin-hTERTp-E1a, Ad-VT) using Apoptin and the hTERT promoter (Xiao et al. 2010). This recombinant adenovirus replicates and expresses Apoptin in tumor cells. Apoptin is a protein that specifically induces apoptosis of tumor cells but has no effect on normal cells. The effect of Apoptin is neither mediated by p53 nor inhibited by overexpression of bcl-2. It is considered a new type of anti-tumor protein. The hTERT promoter is a tumor-specific promoter that can activate some genes in tumor cells and cause them to express genes such as the adenoviral promoter E1a gene and the gene encoding Apoptin in this case. The presence of Apoptin and hTERT promoters can effectively improve the targeting of oncolytic adenovirus and further improve the anti-tumor therapeutic effect.

Currently, combinations of oncolytic adenoviruses and chemotherapy drugs represent an important avenue of research in the treatment of cancer. The main reason is that the combination of chemotherapy drugs and oncolytic adenovirus may not only reduce the toxic side effects of chemotherapy drugs on normal cells, but also increase their inhibitory effects on tumor cells. Through the appropriate combination scheme, chemotherapy drugs will not interfere with the specific recognition of tumor cells by oncolytic adenovirus, nor affect the replication and expression of tumor suppressor genes by the oncolytic adenovirus in tumor cells. The combination of specially constructed oncolytic adenoviruses and chemotherapeutics can treat tumors through their different respective mechanisms of killing the cancer cells. They have synergistic effects, and their cytotoxicity is significantly greater than chemotherapy alone or oncolytic adenovirus alone. Previous studies have shown that cyclophosphamide alone as a drug for the treatment of malignant melanoma failed to reduce tumor growth in mouse models of melanoma, while in contrast, low-dose cyclophosphamide combined with Ad5/3-Δ24-GM-CSF led to complete tumor regression (Hirvinen et al. 2015). The mechanism may be related to the reduction of regulatory T cells (Balkwill 2009) and the inhibitory effect of cyclophosphamide on angiogenesis (Yoo et al. 2007).

In the present paper, the inhibitory effects of Ad-VT, Etoposide and the combination of the two on NCI-H446 cells were studied. The optimal concentration of the combination of Ad-VT and Etoposide was selected. Both Ad-VT and Etoposide had inhibitory effects on NCI-H446 cells with inhibition rates of 43.54% and 26.88% respectively, but a combination of the two achieved greater inhibition, 58.31%, indicating significant synergistic effects. Ad-VT had no significant toxic effect on BEAS-2B cells, unlike Etoposide. However, the toxicity of Etoposide on BEAS-2B cells was significantly reduced when it was administered in combination with Ad-VT. This indicates that the combination could not only enhance tumor inhibitory effects, but also reduce the toxicity of chemotherapy drugs for normal cells. Some studies have shown that Ad-shVEGF, also constructed with adenovirus as the vector, can induce strong anti-tumor angiogenesis in tumor-bearing mice, thus inhibiting tumor (Wang et al. 2011). Another study showed that in the severe combined immunodeficiency mouse renal cancer model established using the cell line TOS-3LN, intra-tumoral injection of Axd Ad B-3 and intraperitoneal injection of gemcitabine (120 mg/kg), resulted in a more significant killing effect on tumor cells and tumor growth inhibition than either agent alone. In the present study, Ad-VT combined with Etoposide was used to inhibit tumor growth in vivo. Compared with the single-drug group, inhibition of tumor growth and survival of tumor-bearing mice in the combined group were

significantly increased. These results suggest that Ad-VT combined with Etoposide can significantly inhibit tumor growth and improve the survival rate of tumor-bearing mice.

Conclusions

The combination of Ad-VT and Etoposide has a synergistic anti-tumor effect, which increases the inhibition of SCLC growth and reduces the side effects of Etoposide. The combination of Ad-VT and Etoposide can inhibit the migration and invasion of tumor cells. The combination of Ad-VT and Etoposide induces apoptosis of cancer cells through mitochondrial membrane potential depolarization. These results provide a theoretical basis for treatment of SCLC using oncolytic adenovirus combined with chemotherapy.

Acknowledgements The authors would like to express their gratitude to EditSprings (https://www.editsprings.cn/) for the expert linguistic services provided.

Author contributions Conceived and designed the experiments: TL, XL, LS and GZ. Performed the experiments: TL, JC, YL, XL, YZ, GS, SL, ZX, YL, and NJ. Analyzed the data: TL, XL, LS and GZ. Contributed reagents/materials/analysis tools: YL, XL, YZ, SL, ZX, ZX, and TL. Wrote the paper: TL and XL. All the authors read and approved the final manuscript.

Funding This work was supported by the Jilin Province Youth Scientific and Technological Talent Support Project (Grant No. QT202111).

Availability of data and materials The datasets used and/or analyzed during the current study are available from the corresponding author on reasonable request.

Declarations

Conflict of interest The authors declare that they have no conflict of interests.

Ethics approval and consent to participate The animal study was reviewed and approved by the Institutional Animal Care and Use Committee (IACUC) of the Changchun University of Chinese Medicine.

Consent for publication Not applicable.

References

Antonia SJ, Lopez-Martin JA, Bendell J, Ott PA, Taylor M, Eder JP, Jager D, Pietanza MC, Le DT, de Braud F, Morse MA, Ascierto PA, Horn L, Amin A, Pillai RN, Evans J, Chau I, Bono P, Atmaca A, Sharma P, Harbison CT, Lin CS, Christensen O, Calvo E (2016) Nivolumab alone and nivolumab plus ipilimumab in recurrent small-cell lung cancer (CheckMate 032): a multicentre, open-label, phase 1/2 trial. Lancet Oncol 17:883–895

Bade BC, Dela Cruz CS, Cancer L (2020) Epidemiology, etiology, and prevention. Clin Chest Med 41(2020):1–24

Balkwill F (2009) Tumour necrosis factor and cancer. Nat Rev Cancer 9:361–371

Bray F, Ferlay J, Soerjomataram I, Siegel RL, Torre LA, Jemal A, Global Cancer Statistics (2018) GLOBOCAN estimates of incidence and mortality worldwide for 36 cancers in 185 countries. CA Cancer J Clin 68(2018):394–424

Byers LA, Rudin CM (2015) Small cell lung cancer: where do we go from here? Cancer 121:664–672

Chiocca EA, Rabkin SD (2014) Oncolytic viruses and their application to cancer immunotherapy. Cancer Immunol Res 2:295–300

Chiocca E, Abbed K, Tatter S, Louis D, Hochberg F, Barker F, Kracher J, Grossman S, Fisher J, Carson K, Rosenblum M, Mikkelsen T, Olson J, Markert J, Rosenfeld S, Nabors L, Brem S, Phuphanich S, Freeman S, Kaplan R, Zwiebel J (2004) A phase I open-label, dose-escalation, multi-institutional trial of injection with an E1B-attenuated adenovirus, ONYX-015, into the peritumoral region of recurrent malignant gliomas, in the adjuvant setting. Mol Ther J Am Soc Gene Ther 10:958–966

Danen-Van Oorschot AAAM, Zhang YH, Leliveld SR, Rohn JL, Seelen MCMJ, Bolk MW, Van Zon A, Erkeland SJ, Abrahams JP, Mumberg D, Noteborn MHM (2003) Importance of nuclear localization of apoptin for tumor-specific induction of apoptosis. J Biol Chem 278:27729–27736

Fruh M, De Ruysscher D, Popat S, Crino L, Peters S, Felip E, E.G.W. Group (2013) Small-cell lung cancer (SCLC): ESMO clinical practice guidelines for diagnosis, treatment and follow-up. Ann Oncol 24(Suppl 6):vi99–vi105

Fulci G, Chiocca E (2003) Oncolytic viruses for the therapy of brain tumors and other solid malignancies: a review. Front Biosci 8:e346-360

Gu D, Kelly TN, Wu X, Chen J, Samet JM, Huang JF, Zhu M, Chen JC, Chen CS, Duan X, Klag MJ, He J (2009) Mortality attributable to smoking in China. N Engl J Med 360:150–159

Heilman DW, Teodoro JG, Green MR (2006) Apoptin nucleocytoplasmic shuttling is required for cell type-specific localization, apoptosis, and recruitment of the anaphase-promoting complex/cyclosome to PML bodies. J Virol 80:7535–7545

Hirvinen M, Rajecki M, Kapanen M, Parviainen S, Rouvinen-Lagerström N, Diaconu I, Nokisalmi P, Tenhunen M, Hemminki A, Cerullo V (2015) Immunological effects of a tumor necrosis factor alpha-armed oncolytic adenovirus. Hum Gene Ther 26:134–144

Kemeny N, Brown K, Covey A, Kim T, Bhargava A, Brody L, Guilfoyle B, Haag N, Karrasch M, Glasschroeder B, Knoll A, Getrajdman G, Kowal K, Jarnagin W, Fong Y (2006) Phase I, open-label, dose-escalating study of a genetically engineered herpes simplex virus, NV1020, in subjects with metastatic colorectal carcinoma to the liver. Hum Gene Ther 17:1214–1224

Liu L, Wu W, Zhu G, Liu L, Guan G, Li X, Jin N, Chi B (2012) Therapeutic efficacy of an hTERT promoter-driven oncolytic adenovirus that expresses apoptin in gastric carcinoma. Int J Mol Med 30:747–754

Ng KK, Vauthey JN, Pawlik TM, Lauwers GY, Regimbeau JM, Belghiti J, Ikai I, Yamaoka Y, Curley SA, Nagorney DM, Ng IO, Fan ST, Poon RT, C. International Cooperative Study Group on Hepatocellular (2005) Is hepatic resection for large or multinodular hepatocellular carcinoma justified? Results from a multi-institutional database. Ann Surg Oncol 12:364–373

Noteborn MH, Koch G (1995) Chicken anaemia virus infection: molecular basis of pathogenicity. Avian Pathol J WVPA 24:11–31

Noteborn MHM, De Boer GF, Van Roozelaar DJ, Karreman C, Kranenburg O, Vos JG, Jeurissen SHM, Hoeben RC, Zantema A, Koch G, Van Ormondt H, Van Der Eb AJ (1991) Characterization of cloned chicken anemia virus DNA that contains all elements for the infectious replication cycle. J Virol 65:3131–3139

Noteborn MH, Todd D, Verschueren CA, deGauw HW, Curran WL, Veldkamp S, Douglas AJ, McNulty MS, van der EA, Koch G (1994) A single chicken anemia virus protein induces apoptosis. J Virol 68:346–351

Phenix KV, Meehan BM, Todd D, McNulty MS (1994) Transcriptional analysis and genome expression of chicken anaemia virus. J Gen Virol 75(Pt 4):905–909

Qi Y, Guo H, Hu N, He D, Zhang S, Chu Y, Huang Y, Li X, Sun L, Jin N (2014) Preclinical pharmacology and toxicology study of Ad-hTERT-E1a-Apoptin, a novel dual cancer-specific oncolytic adenovirus. Toxicol Appl Pharmacol 280:362–369

Qian Y, Yang L, Cao S (2014) Telomeres and telomerase in T cells of tumor immunity. Cell Immunol 289:63–69

Reed LJ, Meunch H (1938) A simple method of estimating fifty percent endpoints. Am J Hyg 27:493–497

Rohn JL, Zhang YH, Aalbers RIJM, Otto N, Den Hertog J, Henriquez NV, Van de Velde CJH, Kuppen PJK, Mumberg D, Donner P, Noteborn MHM (2002) A tumor-specific kinase activity regulates the viral death protein apoptin. J Biol Chem 277:50820–50827

Sato-Dahlman M, Yamamoto M (2018) The development of oncolytic adenovirus therapy in the past and future—for the case of pancreatic cancer. Curr Cancer Drug Targets 18:153–161

Sung H, Ferlay J, Siegel RL, Laversanne M, Soerjomataram I, Jemal A, Bray F (2021) GLOBOCAN estimates of incidence and mortality worldwide for 36 cancers in 185 countries. CA Cancer J Clin 71:209–249

Umar A, Dunn BK, Greenwald P (2012) Future directions in cancer prevention. Nat Rev Cancer 12:835–848

Wang H, Satoh M, Chen GP, Li DC, Hamada H, Arai Y (2011) E1A, E1B double-restricted adenovirus enhances the cytotoxicity and antitumor activity of gemcitabine to renal cell carcinoma. Chin Med J 124:1082–1087

Xiao L, Yan L, Zhongmei W, Chang L, Huijun L, Mingyao T, Kuoshi J, Lili S, Pegn G, Encheng Y, Xiaohong X, Shifu K, Zhuoyue W, Yuhang W, Ningyi J (2010) Potent anti-tumor effects of a dual specific oncolytic adenovirus expressing apoptin in vitro and in vivo. Mol Cancer 9:10

Yang G, Meng X, Sun L, Hu N, Jiang S, Sheng Y, Chen Z, Zhou Y, Chen D, Li X, Jin N (2015) Antitumor effects of a dual cancer-specific oncolytic adenovirus on colorectal cancer in vitro and in vivo. Exp Ther Med 9:327–334

Yoo JY, Kim JH, Kwon YG, Kim EC, Kim NK, Choi HJ, Yun CO (2007) VEGF-specific short hairpin RNA-expressing oncolytic adenovirus elicits potent inhibition of angiogenesis and tumor growth. Mol Ther 15:295–302

Zhang M, Wang J, Li C, Hu N, Wang K, Ji H, He D, Quan C, Li X, Jin N, Li Y (2013) Potent growth-inhibitory effect of a dual cancer-specific oncolytic adenovirus expressing apoptin on prostate carcinoma. Int J Oncol 42:1052–1060

Zhang D, Xiao YF, Zhang JW, Xie R, Hu CJ, Tang B, Wang SM, Wu YY, Hao NB, Yang SM (2015) miR-1182 attenuates gastric cancer proliferation and metastasis by targeting the open reading frame of hTERT. Cancer Lett 360:151–159